Supplementary Fig.1

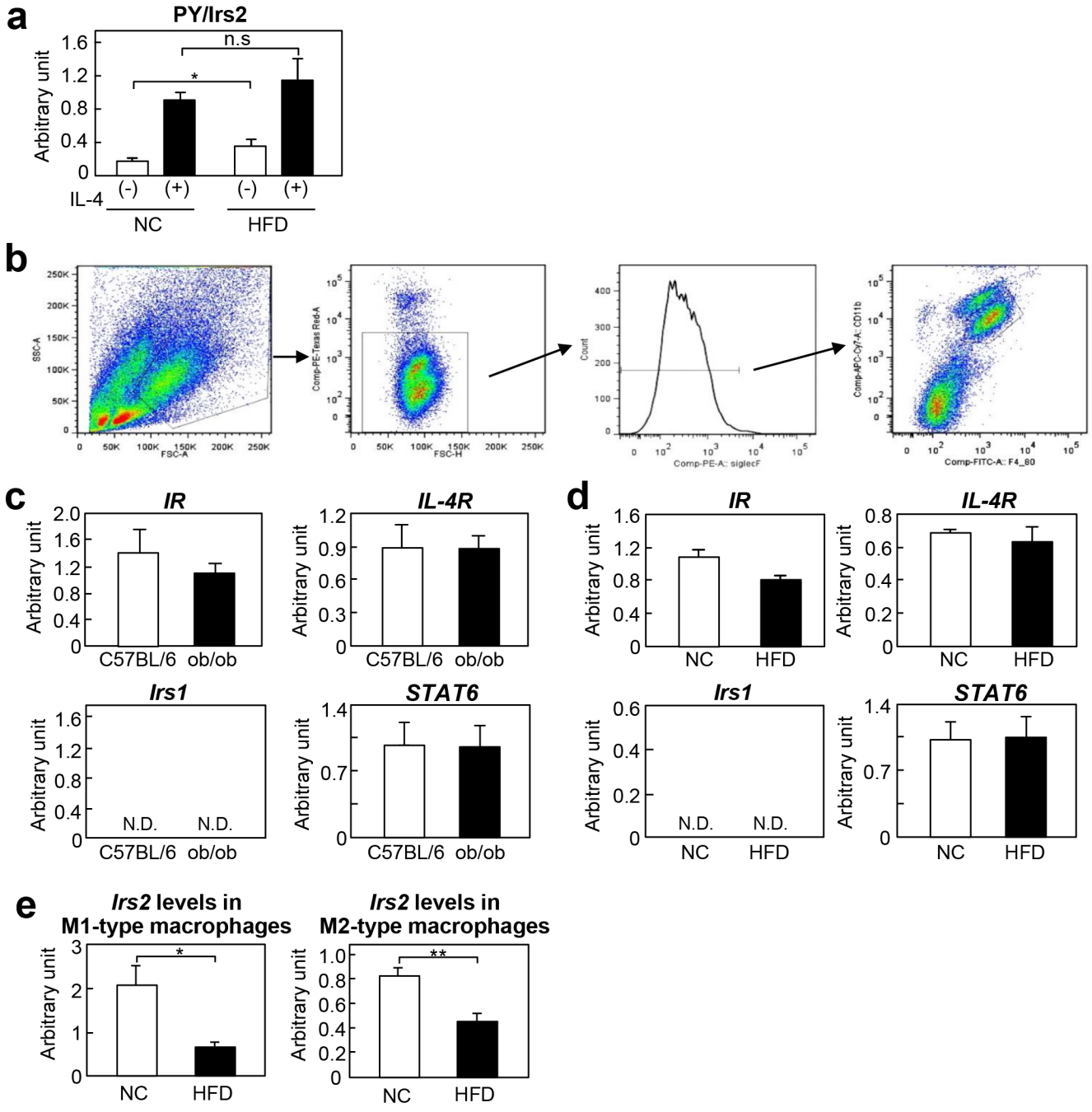

Expression levels in MΦs isolated from the SVF of the adipose tissue of the ob/ob and HF diet-fed mice.
(**a**) Phosphorylation/protein levels of Irs2 in peritoneal MΦs derived from NC and HF diet-fed mice (n = 4). (**b**) Isolation of siglecF$^-$CD11b$^+$F4/80$^+$cells from the SVF of the adipose tissue by flow cytometry. (**c, d**) Expression levels of *IR*, *IL-4R*, *Irs1* and *STAT6* mRNA in the siglecF$^-$CD11b$^+$F4/80$^+$ cells isolated from the SVF of the adipose tissue of the ob/ob and HF diet-fed mice (n = 4). (**e**) Expression levels of *Irs2* in M1-type and M2-type MΦs from NC and HF diet-fed mice (n = 3-7). N.D. is "not-detected". Data are mean±SEM. followed by one-way ANOVA with a *post-hoc* test or Student's *t* test. *, $P < 0.05$; **, $P < 0.01$.

Supplementary Fig.2

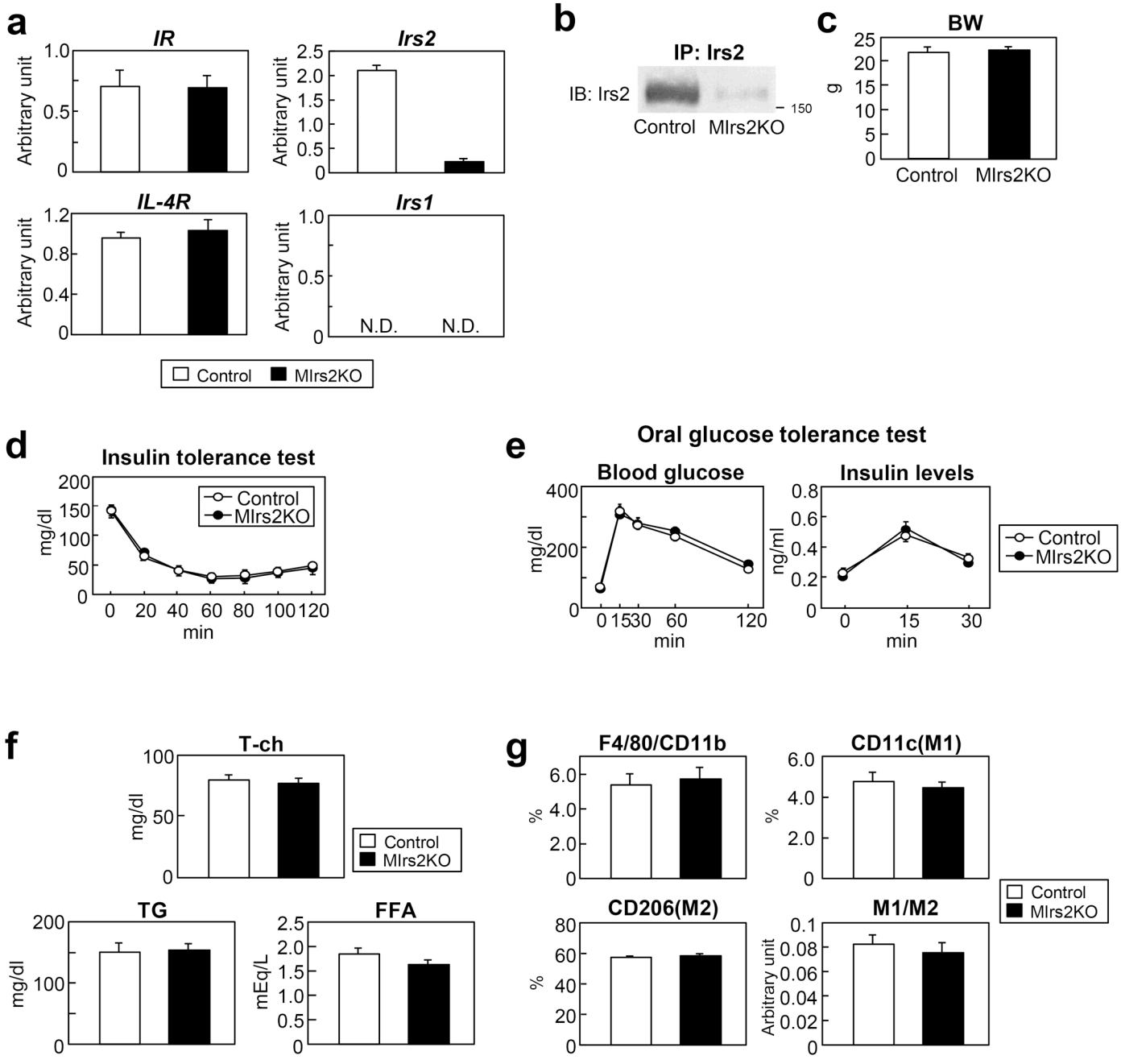

Phenotypes of M*Irs2*KO mice under the NC diet condition.
(**a**) mRNA expression levels of *IR*, *IL-4R*, *Irs1* and *Irs2* in the BMDM of the control and M*Irs2*KO mice (n = 6). (**b**) Irs2 protein levels in the BMDM of the control and M*Irs2*KO mice. (**c-f**) Body weight (BW), insulin tolerance test results (ITT), oral glucose tolerance test results (OGTT) and lipid profiles of the control and M*Irs2*KO mice under the normal chow (NC) diet condition (n = 6-9). (**g**) Percentages of siglecF-CD11b+F4/80+ cells, siglecF-CD11b+F4/80+CD11c+ cells and siglecF-CD11b+F4/80+CD206+ cells in the SVF of the adipose tissue derived from the NC diet-fed M*Irs2*KO mice (n = 4-6). N.D. is “not-detected”. Data are mean±SEM. followed by Student’s t test.

Supplementary Fig.3

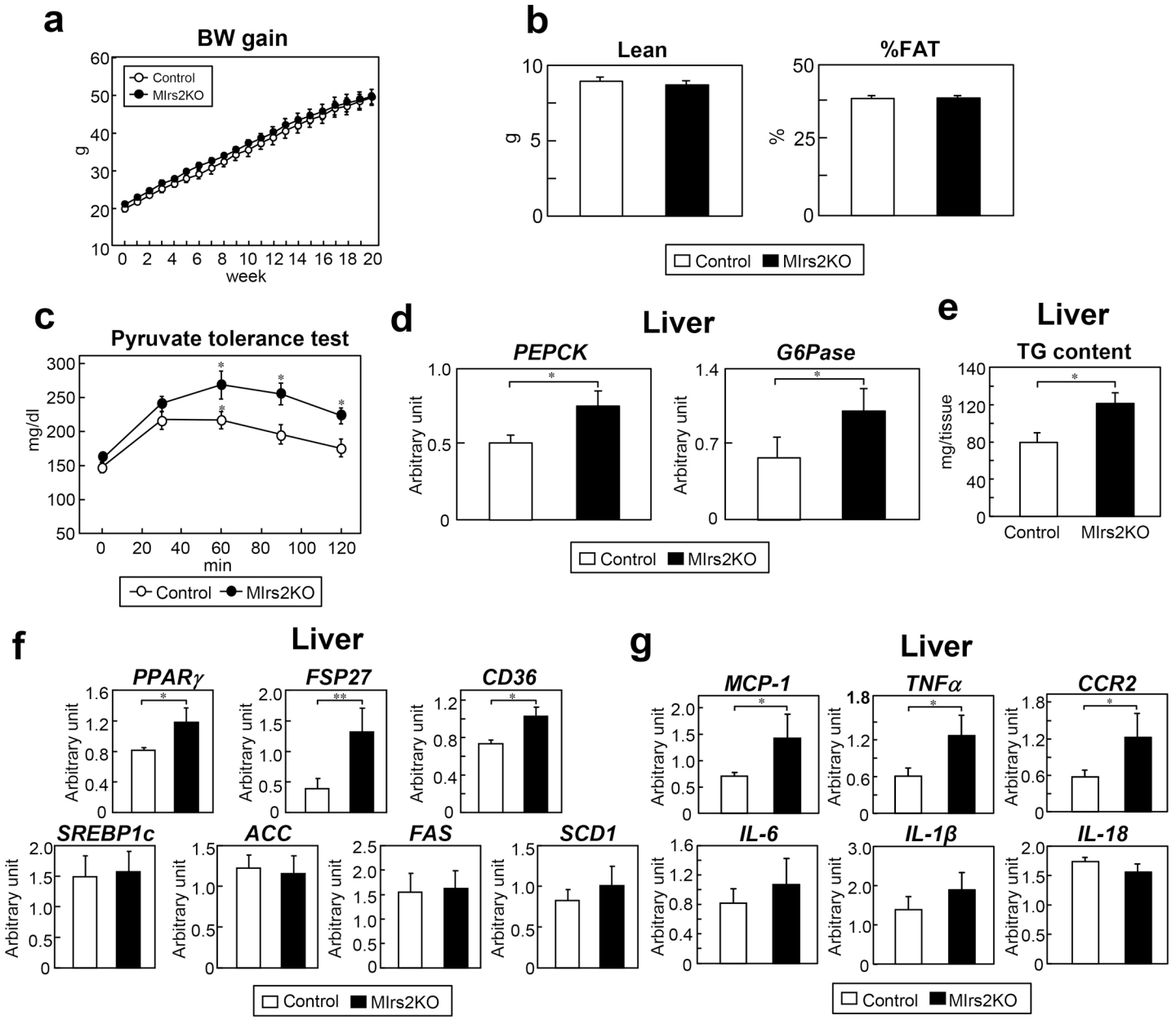

Gluconeogenesis and lipogenesis in the liver of M*Irs2*KO mice under the HF diet condition

(**a**, **b**) BW gain, lean body mass and percent body fat (%FAT) of the control and M*Irs2*KO mice reared on a HF diet (n = 8-9). (**c**) Pyruvate tolerance test in the M*Irs2*KO mice (n = 7-9). (**d**) Expression levels of gluconeogenesis-associated genes in the M*Irs2*KO mice under the HF diet condition (n = 9-10). (**e**) Hepatic TG content in the M*Irs2*KO mice (n = 5). (**f**) Expression levels of lipogenesis-associated genes in the M*Irs2*KO mice under the HF diet condition (n = 9-10). (**g**) Quantitative RT-PCR analysis of the genes encoding inflammatory cytokines in the livers of the M*Irs2*KO mice (n = 9-10). N.D. is "not-detected". Data are mean±SEM. followed by Student's t test. *, $P < 0.05$; **, $P < 0.01$.

Supplementary Fig.4

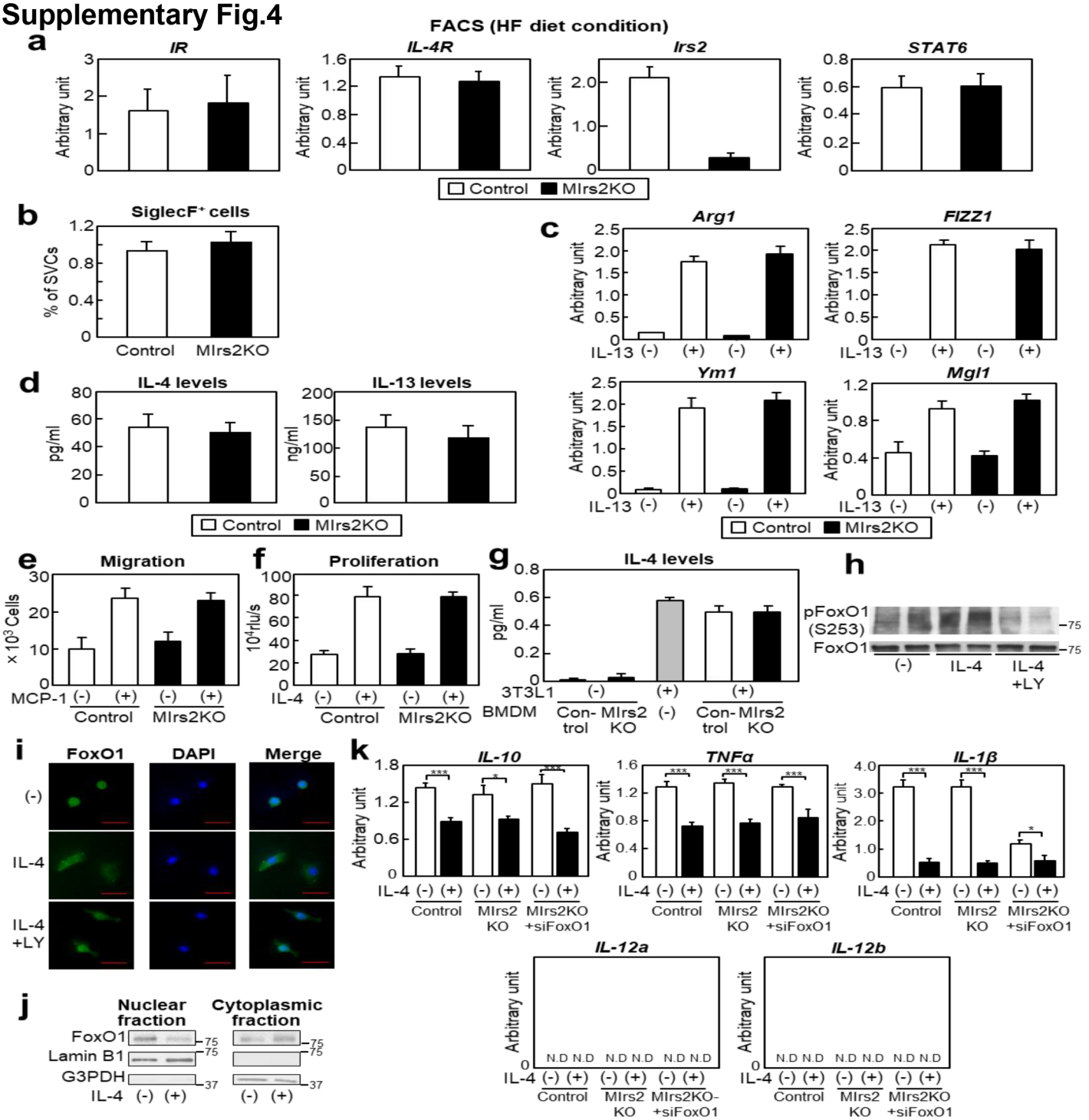

The role of FoxO1 in M2a-subtype MΦ after IL-4 stimulation.

(**a**) *IR*, *IL-4R*, *Irs2* and *STAT6* expression levels in the siglecF-CD11b+F4/80+ cells of M*Irs2*KO mice reared on a HF diet (n = 10-14). (**b**) The percentage of SiglecF+ cells in the SVCs of M*Irs2*KO mice fed a HF diet (n = 9-11). (**c**) Expression levels of the M2a-subtype MΦ marker genes in the BMDM of the control and M*Irs2*KO mice 48h after IL-13 stimulation (n = 3). (**d**) IL-4 and IL-13 levels in the WAT of the control and M*Irs2*KO mice (n = 5). (**e**) Migration of the BMDM of the control and M*Irs2*KO mice 48h after MCP-1 stimulation (n = 5-10). (**f**) Proliferation of the BMDM of the control and M*Irs2*KO mice 48h after IL-4 stimulation (n = 5-6). (**g**) IL-4 levels in the conditioned medium after co-culture of BMDM of M*Irs2*KO mice with or without 3T3-L1 cells for 24 h (n = 7-9). (**h**) FoxO1 phosphorylation and protein expression levels in the BMDM of the C57BL/6 mice after IL-4 stimulation with LY294002 treatment. (**i**) Immunohistochemical staining for FoxO1 in the BMDM of the C57BL/6 mice after IL-4 stimulation with LY294002 treatment (scale bar, 50 μm). (**j**) FoxO1 protein expression of nuclear and cytoplasmic fractions in the BMDM of the C57BL/6 mice after IL-4 stimulation. (**k**) Expression levels of *IL-10*, *TNFα*, *IL-1β*, *IL-12a*, and *IL-12b* in the siFoxO1-transfected BMDM of the M*Irs2*KO mice after IL-4 stimulation (n = 4-10). N.D. is "not-detected". Data are mean±SEM. followed by one-way ANOVA with a post-hoc test or Student's t test. *, $P < 0.05$; ***, $P < 0.001$.

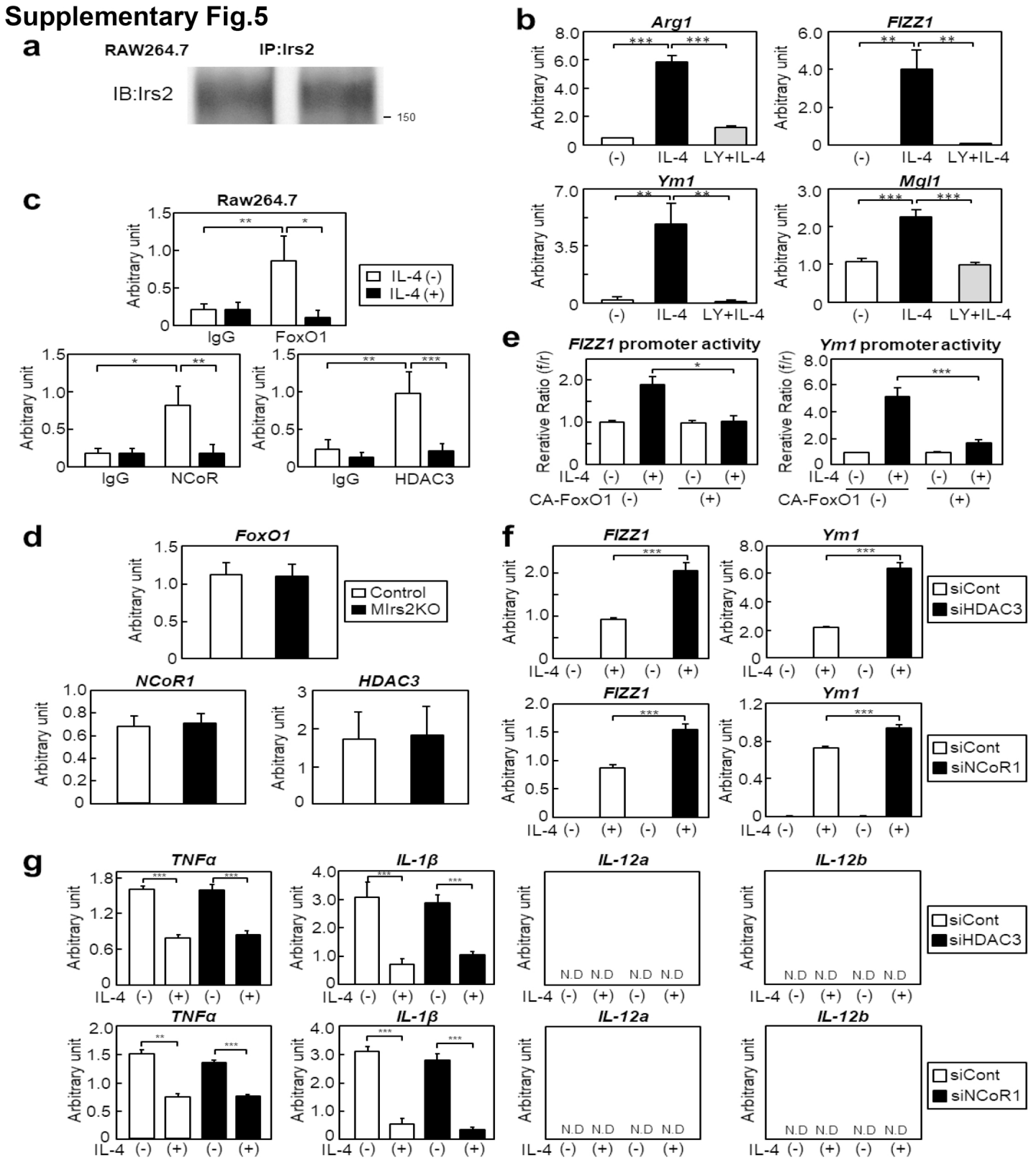

IL-4-induced *FIZZ1* and *Ym1* expressions were increased by the dissociation of the FoxO1/HDAC3/NCoR1 corepressor complex. (**a**) Irs2 protein expression in the RAW264.7 cells. (**b**) Expression levels of the M2a-subtype MΦ marker genes in the RAW264.7 cells after IL-4 stimulation with LY294002 treatment (n = 3). (**c**) Chip-qPCR using FoxO1, HDAC3 and NCoR1 antibody in the RAW264.7 cells before and after IL-4 stimulation (n = 5-10). (**d**) FoxO1, HDAC3 and NCoR1 expression levels in the ATMs of control and M*Irs2*KO mice (n = 12-15). (**e**) *FIZZ1* and *Ym1* promoter activities after IL-4 stimulation with or without CA-FoxO1 transfection (n = 4-5). (**f**) Expression levels of *FIZZ1* and *Ym1* in the BMDM of the C57BL/6 mice after IL-4 stimulation with siHDAC3 or siNCoR1 transfection (n = 3-8). (**g**) Expression levels of *TNFα*, *IL-1β*, *IL-12a*, and *IL-12b* in siHDAC3- or siNCoR1-transfected BMDM of the C57BL/6 mice after IL-4 stimulation (n = 3-8). N.D. is "not-detected". Data are mean±SEM. followed by one-way ANOVA with a post-hoc test or Student's t test. *, $P < 0.05$; **, $P < 0.01$; ***, $P < 0.001$.

Supplementary Fig.6

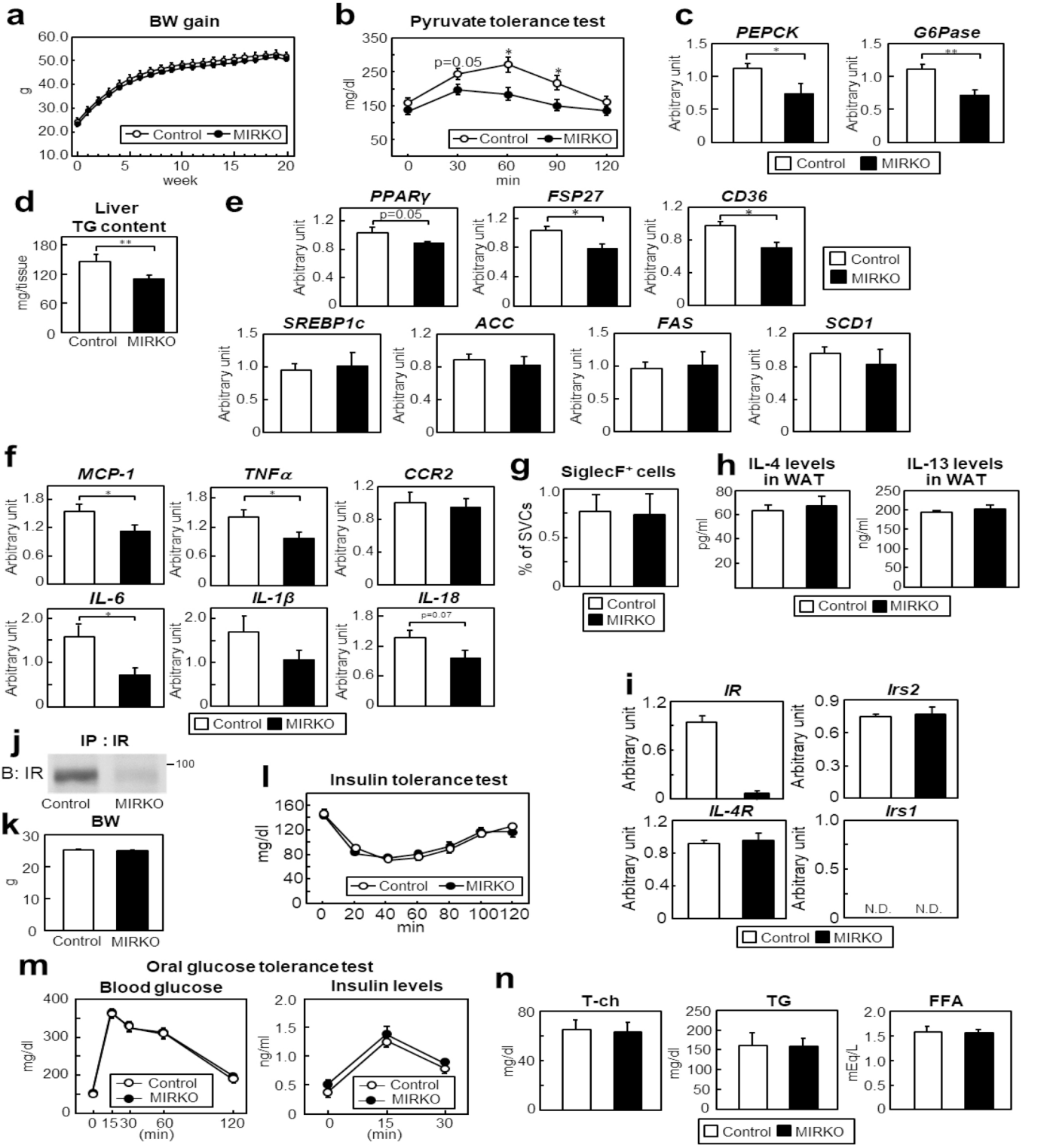

Phenotypes of M*IR*KO mice under the NC and HF diet condition.

(**a**) BW gain in the control and M*IR*KO mice reared on a HF diet (n = 9-10). (**b**) Pyruvate tolerance test in the M*IR*KO mice (n = 8). (**c**) Expression levels of gluconeogenesis-associated genes in the HF diet-fed M*IR*KO mice (n = 6-8). (**d**) Hepatic TG content in the M*IR*KO mice (n = 4-5). (**e**) Expression levels of lipogenesis-associated genes in the HF diet-fed M*IR*KO mice (n = 6-8). (**f**) Quantitative RT-PCR analysis of the genes encoding inflammatory cytokines in the livers of the M*IR*KO mice (n = 6-8). (**g**) The percentage of SiglecF+ cells in the SVCs of M*IR*KO mice fed a HF diet (n = 4-5). (**h**) IL-4 and IL-13 levels in the WAT of the control and M*IR*KO mice (n = 5). (**i**) mRNA expression levels of *IR*, *IL-4R*, *Irs1* and *Irs2* in the BMDM of the control and M*IR*KO mice (n = 9-10). (**j**) IR protein levels in the BMDM of the control and M*IR*KO mice. (**k-n**) Body weight (BW), insulin tolerance test (ITT) results, oral glucose tolerance test (OGTT) results and lipid profiles in the control and M*IR*KO mice under the NC diet condition (n = 6-10). N.D. is "not-detected". Data are mean±SEM. followed by Student's t test. *, $P < 0.05$; **, $P < 0.01$.

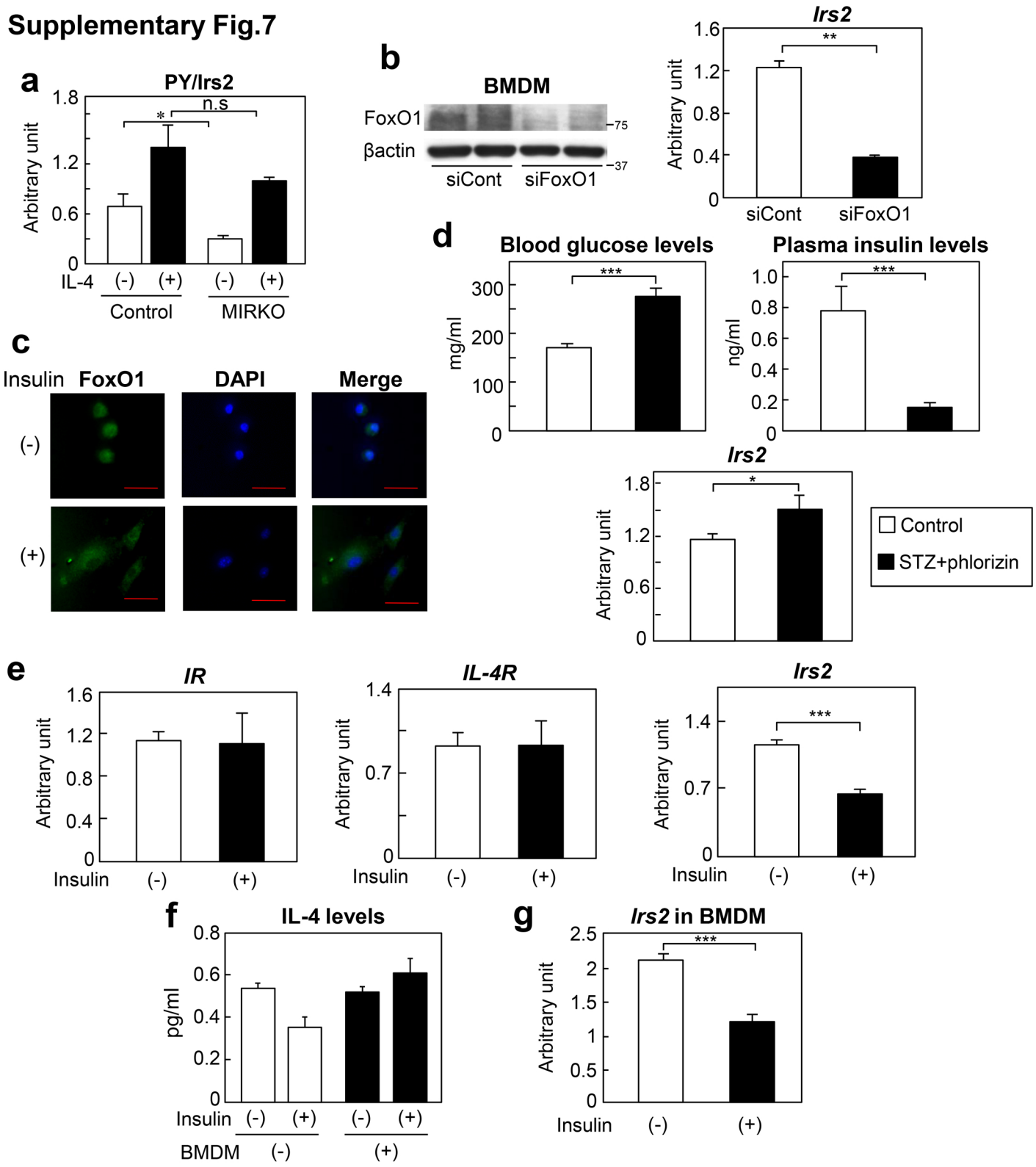

Expression levels of *Irs2* in MΦs after insulin stimulation.

(**a**) Phosphorylation/protein levels of Irs2 in the peritoneal MΦs of HF diet-fed M*IR*KO mice (n = 3-6). (**b**) *Irs2* expression levels in the BMDM after siFoxO1 transfection (n = 6). (**c**) Immunohistochemical staining for FoxO1 in the BMDM after insulin stimulation (scale bar, 50 μm). (**d**) Blood glucose levels, plasma insulin levels and expression levels of *Irs2* in the peritoneal MΦs in mice after STZ plus phlorizin treatment (n = 5-10). (**e**) Expression levels of *IR*, *IL-4R*, and *Irs2* in the BMDM 3 h after insulin stimulation (n = 8-10). (**f**) IL-4 levels in the conditioned medium after co-culture of BMDM and 3T3-L1 cells after insulin stimulation for 24 h (n = 6). (**g**) *Irs2* expression levels in BMDM co-cultured with 3T3-L1 cells after insulin stimulation for 24 h (n = 11-20). Data are mean±SEM. followed by one-way ANOVA with a post-hoc test or Student's t test. *, $P < 0.05$; **, $P < 0.01$; ***, $P < 0.001$.

Supplementary Fig.8

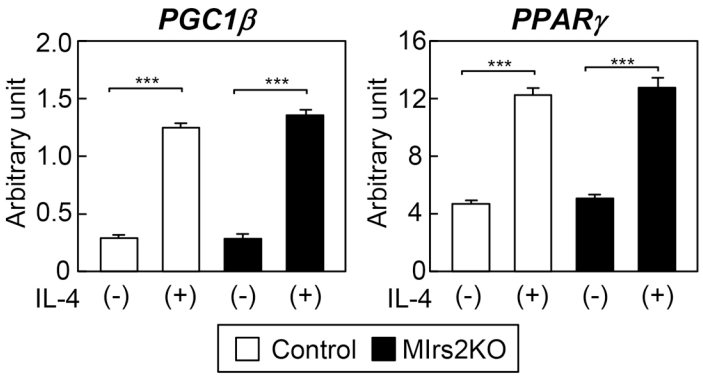

PGC1β and *PPARγ* expression levels did not differ between the control and M*Irs2*KO mice after IL-4 treatment.
Expression levels of *PGC1β* and *PPARγ* in the BMDM of the control and M*Irs2*KO mice after IL-4 stimulation (n = 6-8). Data are mean±SEM. followed by Student's t test. ***, $P < 0.001$.

Supplementary Fig.9

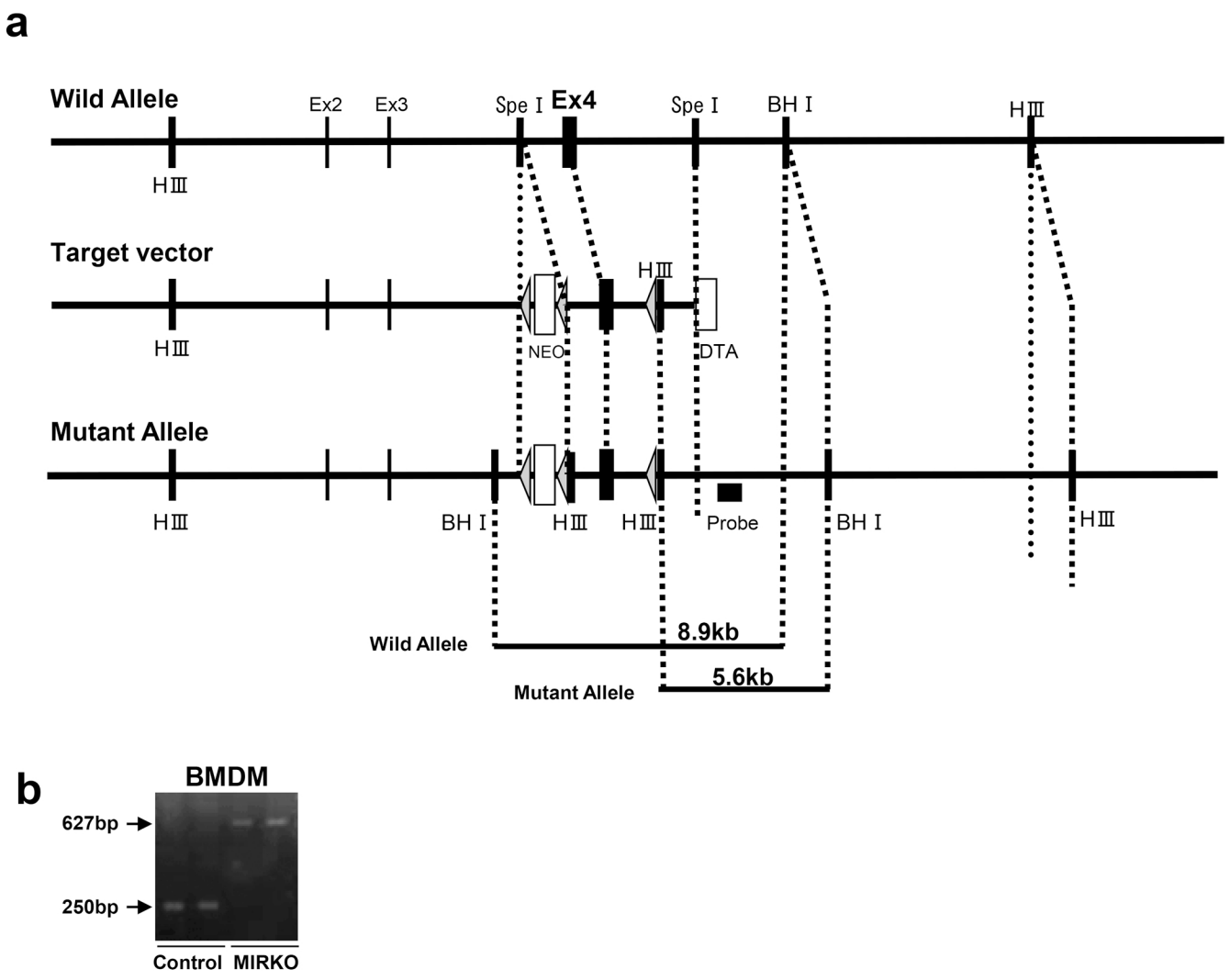

Generation of M*IR*KO mice

(**a**) Targeting strategy to insert LoxP sites into the *IR* gene. (**b**) PCR analysis of genomic DNA in MΦs to detect Cre-mediated recombination in the M*IR*KO mice.

Supplementary Fig.10

Fig.1a

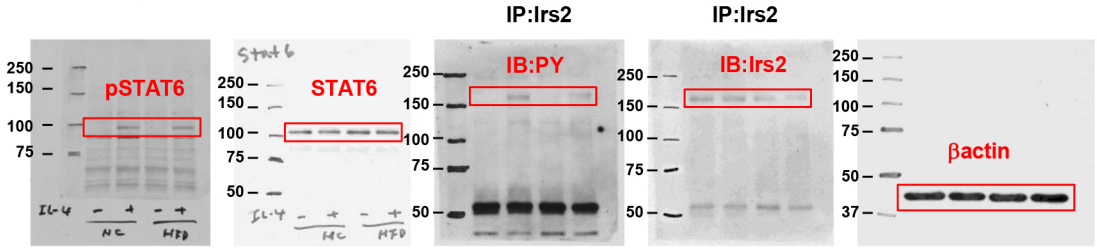

Fig.1f

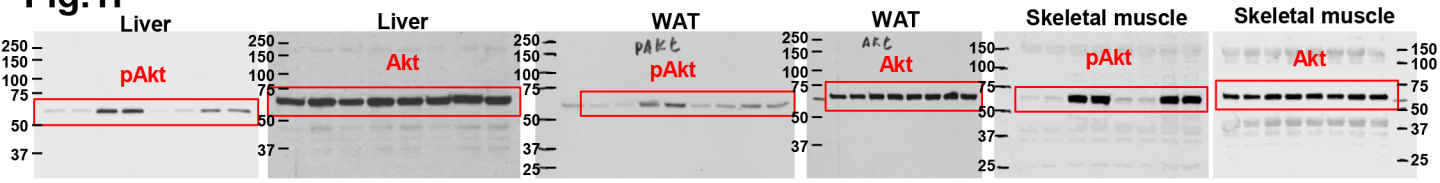

Fig. 2g

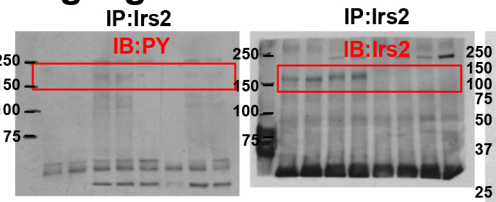

Fig. 2h

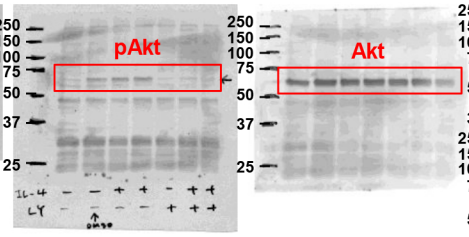

Fig. 2i

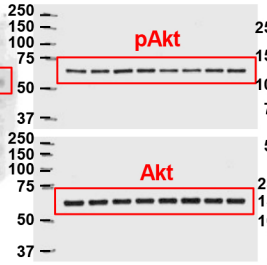

Fig. 2l

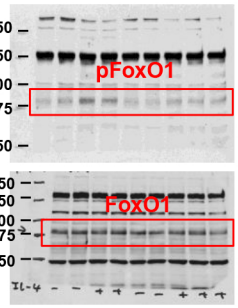

Fig. 3c

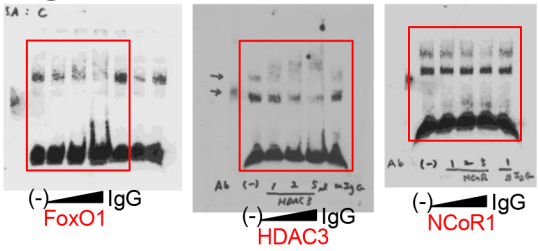

Fig. 3f

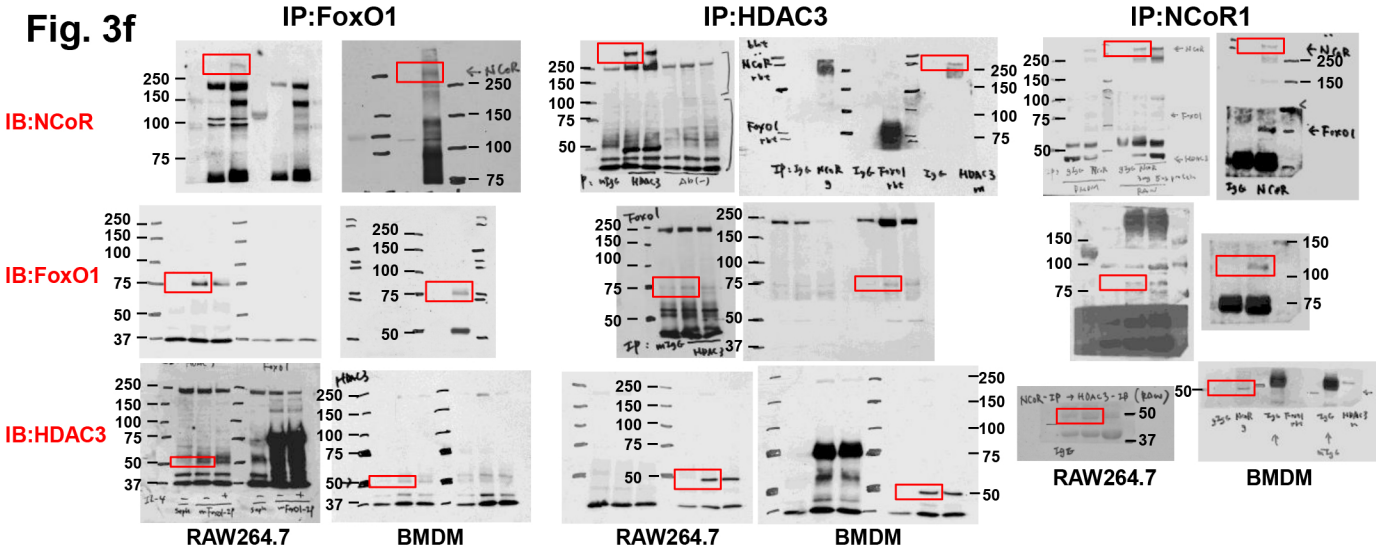

Fig. 4c

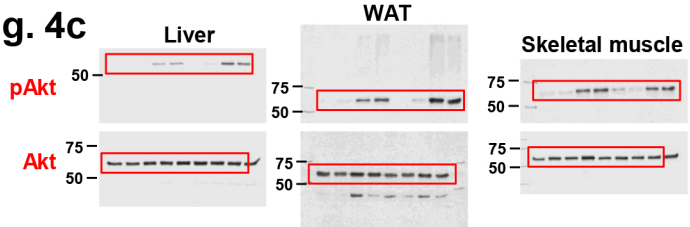

Uncropped images of immunoblot data.

Supplementary Fig.11

Fig.5b

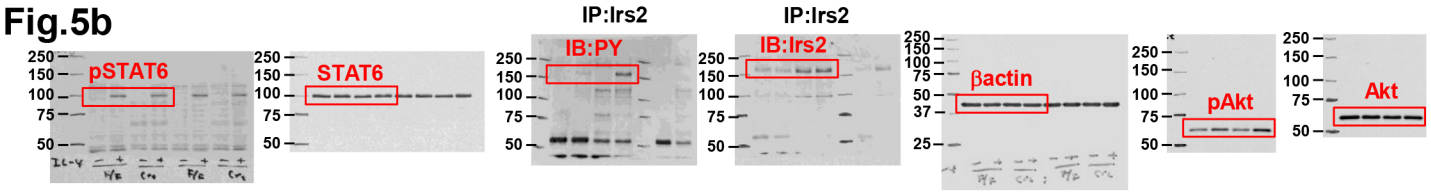

Fig. 6a

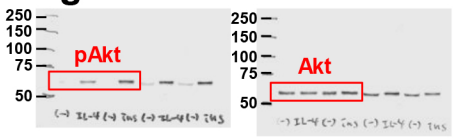

Fig. 6c

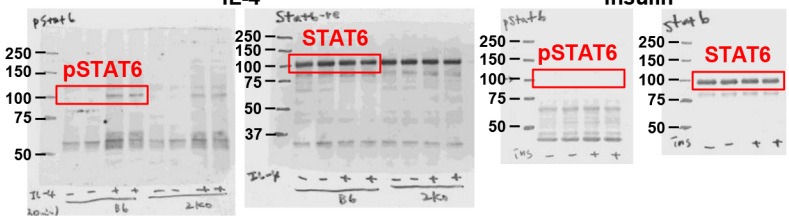

Fig. 6d

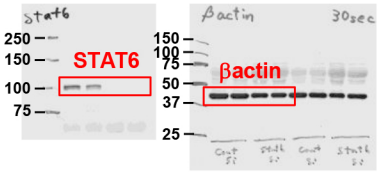

Fig. 6e

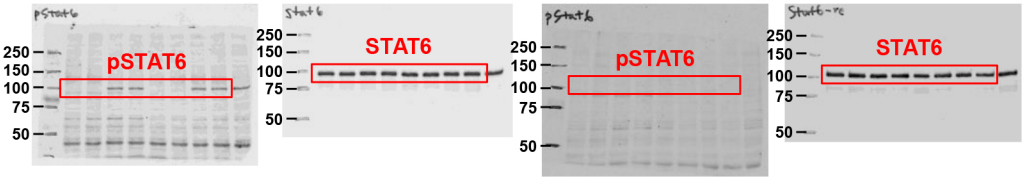

Fig. 6f

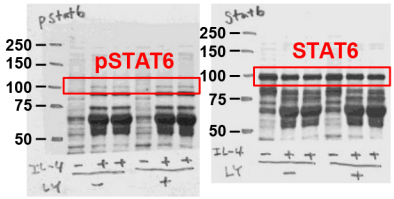

SFig. 2b

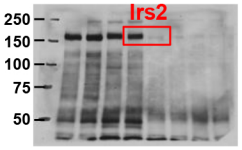

SFig. 4h

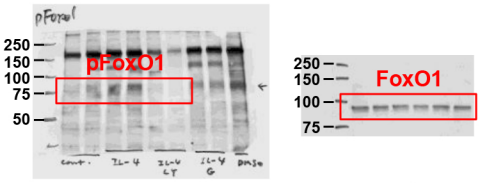

SFig. 4j

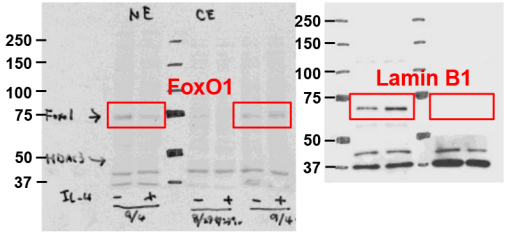

SFig. 5a

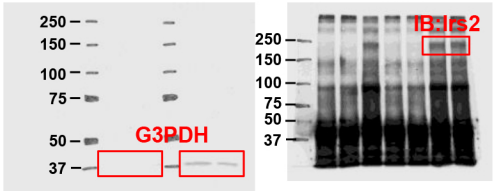

SFig. 6j

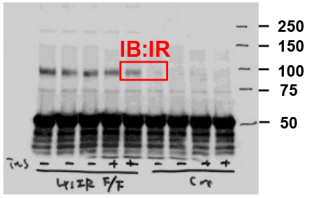

SFig. 7b

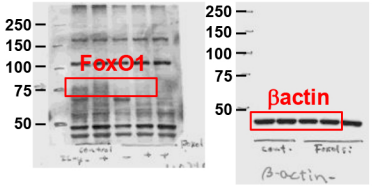

SFig9b

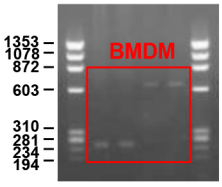

Uncropped images of immunoblot and PCR data.